Determination of fission barrier height of ^{210}Fr and ^{210}Ra via neutron measurement

M. Veselský,[*] P. Rubovič, V. Petousis,[†] H. Natal da Luz, P. Burian, P. Mánek, L. Meduna, and P. Smolyanskiy
Institute of Experimental and Applied Physics, Czech Technical University, Husova 240/5, 11000 Prague, Czechia

R. Raabe, A. Camaiani, J. Klimo, O. Poleshchuk, A. Youssef, A. Ceulemans, and M. Latif
KU Leuven, Instituut voor Kern- en Stralingsfysica, Celestijnenlaan 200d, 3001 Leuven, Belgium

M. Jandel
Department of Physics and Applied Physics, University of Massachusetts Lowell, Lowell, Massachusetts 01854, USA

M. Bírová, A. Herzán, A. Špaček, and M. Venhart
Institute of Physics, Slovak Academy of Sciences, Dúbravská cesta 9, 845 11 Bratislava, Slovakia

M. G. Pellegriti
INFN Catania, Via Santa Sofia 64, 95123 Catania, Italy

A. N. Andreyev and C. Page
School of Physics, Engineering and Technology, University of York, Heslington, York YO10 5DD, United Kingdom

G. A. Souliotis
Laboratory of Physical Chemistry, Department of Chemistry, National and Kapodistrian University of Athens, Zografou, 157 71 Athens, Greece

R. Lica
ISOLDE, CERN, Espl. des Particules 1, 1211 Meyrin, Switzerland
and Horia Hulubei National Institute for Physics and Nuclear Engineering - IFIN-HH, R-077125, Bucharest, Romania

(Received 17 May 2023; revised 4 December 2023; accepted 22 December 2023; published 18 January 2024)

Fission barrier heights of short-lived nuclei away from line of β stability are not known reliably. Low-energy fission of ^{210}Fr and ^{210}Ra, produced by (d, p) and (d, n) transfer reaction on the re-accelerated unstable beam ^{209}Fr was investigated at HIE-ISOLDE. Four Timepix3 pixel detectors were installed on the body of the ACTAR TPC demonstrator chamber. Polyethylene converters were used for the detection of fast neutrons. Since no significant background was observed, it was possible to measure the spatial distribution of emitted neutrons reflecting the fission excitation function. Subsequent simulations employing the results of the TALYS code and available data on fission fragment distributions allowed to estimate directly the value of the fission barrier height for the neutron-deficient nucleus ^{210}Fr. This first direct measurement confirmed the reduction of the fission barrier compared to available theoretical calculations by 15–30%.

DOI: 10.1103/PhysRevC.109.014618

I. INTRODUCTION

Nuclear fission is known for more than 80 years ago and represents one of the most dramatic examples of nuclear large-amplitude processes, in which the nucleus splits into two fragments releasing a large amount of energy. Fission is not only important for applications such as energy generation and production of radioisotopes; it has also direct consequences on the synthesis of the heaviest elements in the astrophysical r process, which is terminated by fission, and on the abundance of medium-mass elements in the universe through the so-called "fission recycling" [1–3]. Fission usually occurs when the excitation energy of the nucleus exceeds the fission barrier height. An ideal way to measure fission barrier heights is to study low-energy fission, where excitation energies are comparable to the height of the fission barrier. Recently, low-energy fission was studied in the region from thorium

[*]Martin.Veselsky@cvut.cz
[†]Corresponding author: Vlasios.Petousis@cvut.cz

to fermium, using spontaneous fission, fission induced by neutrons and light stable beams, or β-delayed fission. Most of the reliably known fission barriers were measured in reactions with light stable beams, see, e.g., [4]. Three decades ago, at the radioactive ion beam facility of GSI, a new technique was developed to study low-energy fission in other regions of the nuclear chart [5]. Fission induced by Coulomb excitation of high-energy beams of short-lived radioactive nuclei allowed to observe a transition from asymmetric to symmetric fission as the dominant mode in the neutron-deficient uranium to astatine region. Recently, the probability of the electron-capture delayed fission of ^{178,180}Tl was measured at HIE-ISOLDE and a new asymmetric mode of fission was observed [6].

One of the open questions in fission is the height of the fission barriers of neutron-deficient nuclei. The region between lead and uranium is of special interest, since around the closed neutron shell at $N = 126$ the fission barrier height is strongly influenced by shell structure. Even small differences between predicted and observed fission barrier heights can have implications for the prediction of production rates of superheavy nuclei, where fission barriers exist purely due to shell structure. Statistical model calculations to reproduce the experimental evaporation residue cross sections in this region between lead and uranium, typically led [4,7] to extracted values of fission barrier heights in disagreement with theory, as available theoretical values [8–10] need to be scaled down by 15% to 40%. The measured β-delayed fission probability [6] was also used to deduce the fission barrier height of the daughter isotopes ^{178,180}Hg [11], with deduced values again 10% to 40% smaller than theoretical estimates.

Here, we report on the first measurement of the fission barrier height of a short-lived heavy nucleus, not accessible using stable beam and target nuclei. In reactions induced in inverse kinematics by a post-accelerated radioactive beam of ^{209}Fr nuclei, the yields of neutrons emitted at various angles in subsequent fission processes were used to determine the fission barrier height. This can be considered as a novel method which can find application in further studies.

II. EXPERIMENT

Nuclei of the unstable ^{209}Fr isotope ($t_{1/2} = 50.5$ s) were produced at the HIE-ISOLDE facility in CERN (Geneva, Switzerland) in reactions induced on a UC_x target by the 1.4-GeV proton beam from the PS Booster. The ^{209}Fr atoms were surface-ionized in the target-ion source ensemble, separated through the High-Resolution magnetic Separator (HRS), bunched in REXTRAP, charged-bred in the REX-EBIS ion source and finally post-accelerated through the HIE-ISOLDE linear accelerator [12] to an energy of 7.63 MeV/nucleon. The beam, with an intensity of about 10^6 pps (particles per second) was delivered to the experimental setup, consisting of the ACTAR Demonstrator active target [13] filled with deuterium gas at a pressure of 500 mbar or 800 mbar. The beam entered the gas chamber through a Ti window. Reactions of the ^{209}Fr nuclei of the beam with the deuteron nuclei of the gas could take place at any position along the beam track inside the gas chamber. The gas volume hosted an electric field cage, that allowed the three-dimensional reconstruction of the trajectories of charged particles traversing the gas, by using the principle of a time-projection chamber: the ionisation electrons were collected in the uniform field towards an amplification zone, where their total charge and arrival time were recorded on a pixelated plane. Unfortunately, the results collected by ACTAR Demonstrator active target were affected by the time structure of the delivered beam where beam nuclei were packed in narrow bunches which caused concentration of the volume charge and distortion of the electric field in the active volume. However, the neutron detectors were not affected by this circumstance and here we focus in the detection of neutrons produced in the reactions and subsequent decays in the gas volume.

Four Timepix3 pixel detectors [14] (256×256 pixels with pitch size 55 μm) with 300 μm thick Si sensors were installed on the body of the ACTAR Demonstrator chamber (outside of the gas volume). Timepix3 detectors detect x rays, γ rays, electrons, and charged nuclear particles. The type of radiation can be identified by the different shape of the tracks. Polyethylene converters were used for the detection of fast neutrons, through their scattering on the hydrogen nuclei in the converter; the recoil protons are then identified in the Timepix3 sensors thanks to circular tracks ("blobs"). The thickness of the converters was 1 mm and their density was 0.95 g cm^{-3}. Compared to conventional neutron detectors there is no problem to distinguish neutrons from γ and x rays, due to different shapes of tracks (single pixel hits or curly tracks from secondary electrons). More information on detection of neutrons using Timepix3 detectors can be found, e.g., in [15]. Two detectors (referred to as nos. 1 and 2) were placed on the downstream flange of the chamber, while two more were located on the side flange; one detector (no. 3) upstream and one detector (no. 4) downstream with respect to the incoming beam direction (see Fig. 1). Multiple scattering of neutrons from the ACTAR-TPC chamber is expected to be small as the chamber is made of aluminum and the flanges have a beehive-like structure with frames holding detectors and PCBs with electronics.

The signals from pixels with hits were read out using Katherine readout modules [16]. An example of preselected raw data (cluster size $\geqslant$32) is shown in Fig. 2. Most of the signals are due to electrons, which are scattered multiple times in the Si sensors and leave the characteristic curly tracks. The x rays and γ rays leave single-pixel hits. The tracks of protons recoiling from collisions with fast neutrons were selected by a clusterization software [17] developed at the Institute of Experimental and Applied Physics in Prague, by applying appropriate conditions on size, total energy and shape (roundness) of the tracks. The resulting two-dimensional plot of hits by fast neutrons is shown in Fig. 3. The polyethylene converter covered only the upper 75% of the surface of the detector: this is reflected in the spatial distribution of the recoiling protons.

III. RESULTS AND DISCUSSION

The deuterium gas in the ACTAR TPC Demonstrator was irradiated by the beam of ^{209}Fr nuclei and the yield of fast neutrons emitted in reactions and subsequent decays were measured using Timepix3 detectors with polyethylene

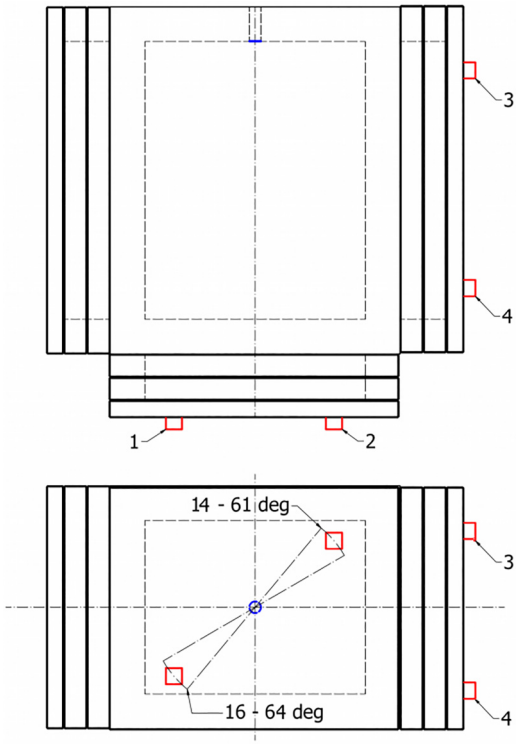

FIG. 1. Positions of the Timepix3 detectors (red) placed on the ACTAR Demonstrator chamber. The Ti entrance window of the beam into the gas volume is indicated in blue. For detectors nos. 1 and 2 the mean polar angle with respect to the beam track is reported for the two extreme cases, i.e., an interaction occurring right after the Ti window (16° and 14°, respectively) and at the end of the chamber (64° and 61°).

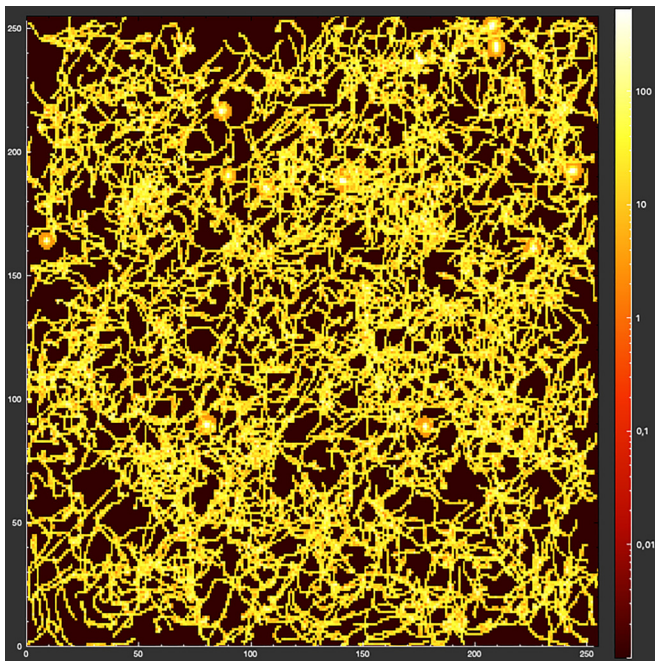

FIG. 2. Tracks of particles detected in Timepix3 detector no. 2 with the polyethylene converter, placed on the downstream flange of the ACTAR Demonstrator chamber. Only tracks with size larger than 32 pixels are plotted. Situation is analogous in all detectors.

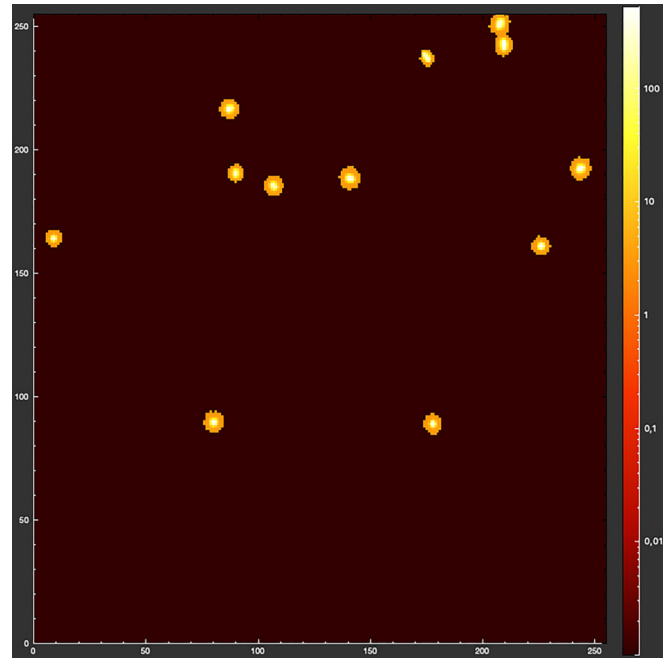

FIG. 3. Tracks of protons ("blobs") recoiling from collisions with fast neutrons, identified among all the signals shown in Fig. 2.

converters. Data were collected for two gas pressures of 500 and 800 mbar. Backgrounds were investigated with beam off and there is no significant fast neutron background, since there is not a feasible source of fast neutrons. The beam nuclei which end up in the beam dump do not decay by spontaneous fission. The possible contribution from cosmic rays is excluded by vertical orientation of detectors. Other possible background can be caused by alpha decay of ^{222}Rn but this was not observed either. Since no significant fast-neutron background was observed in the offline measurements, it was possible to measure the yields of emitted neutrons at various angles quite precisely.

To extract the parameters of the fission channel, detailed simulations were performed. By calculating the energy loss of the beam particles in the deuterium gas by using the SRIM code [18], the beam energy at each position along the beam axis was determined. As initial guess, the results of the TALSY code [19] with a "blind" parameter set (employing only default options) were used to estimate the cross sections of (d, p) and (d, n) channels, which were then used for further analysis. The cross sections of deuterium dissociation was at the level of a few percent and was not considered. Two-body kinematics was applied to the (d, p) and (d, n) reaction channels and the corresponding residual nuclei, ^{210}Fr and ^{210}Ra, respectively. The distribution in excitation energy of the single-particle states of the residual nucleus resulting from one-nucleon transfer was approximated by a flat distribution, as it was done, e.g., in [11] in the case of β-delayed fission. If the excitation energy exceeded the sum of the macroscopic fission barrier height of Sierk [9] with a ground-state shell correction [20], scaled down by 0 to 25%, fission was simulated. The practice to scale fission barriers of even wider range of nuclei is a standard and successful one, as demonstrated, e.g., in the

work [23], where it was applied with success also to the cases of ^{210}Fr and ^{210}Ra. However, even if the same fission barrier scaling is applied to both nuclei, still the latter one can be considered as secondary, since it is even-even and thus uncertainty in pairing gap in saddle point applies and also since due to different excitation function its spatial distribution does not extend into most sensitive region. The resulting neutron yields especially at forward angles reflect primarily properties of ^{210}Fr fission.

The available data on the mass distribution of fission fragments around ^{210}Fr [21] are mass symmetric and the total kinetic energy in the same data suggests that no more than two neutrons can be emitted in the process of fission. These neutrons were emitted isotropically from fission fragments; pre-scission neutron emission was not considered for such low-energy fission. The simulations were performed using a Monte Carlo method and the yields of neutrons in the Timepix3 detectors were estimated using their geometric coverage. The detection efficiency of Timepix3 detectors for fast neutrons is quite low (3×10^{-4}) [22] but it was the same for all detectors. The detection threshold is around 1 MeV what does not affect the neutron detection efficiency due to the boost from fission fragments velocity in inverse kinematics. The simulations were performed for fission barriers from Sierk, corrected for ground state shell corrections, scaled down by 0 to 25% (in steps of 5%, smaller steps would become comparable with experimental statistical uncertainty) and for fission neutron multiplicities between zero and two (in steps of 1). Since the residual nucleus ^{210}Ra in the (d, n) transfer channel is even-even, an assumption had to be made concerning the magnitude of pairing gap in the saddle configuration, which is a quantity not accessible experimentally. The magnitude of pairing gap was varied between 0 and 100% of pairing gap in the ground state. Calculations were performed for both deuterium gas pressures of 500 and 800 mbar.

The relative yields in all four detectors at both pressures were reproduced (within statistical errors) by using a fission barrier scaling factor 0.85 and a fission neutron multiplicity of two. The magnitude of the pairing gap in the saddle configuration of the ^{210}Ra, produced in the (d, n) transfer channel, was at 50% of the ground state value. The results of the simulation with this set of parameters are shown in Figs. 4 and 5. Relative yields of both experimental data and simulations, normalized to the highest yield in detector no. 2, exhibit the same shape. The simulation with a scaling factor 0.85 was the only one which could reproduce the relative yield at both pressures in detector nos. 1 and 2 (those with the highest yields), placed on the downstream flange of the ACTAR Demonstrator chamber. The simulation with the full barrier failed specifically in the case of the higher gas pressure of 800 mbar. The discrepancies in detector nos. 3 and 4, placed at the side of the chamber, are statistically within uncertainties. The background rate was very low (one event per 6 h per detector) and was included only into the lower error bars. The multiplicity of two emitted neutrons appears optimal, and it is not a surprise, since such value can be obtained when taking into account difference of Q value and experimental total kinetic energy, reported in [21].

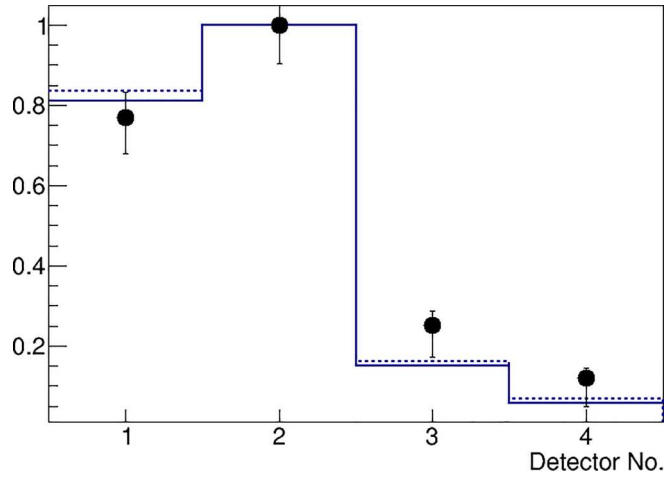

FIG. 4. Relative neutron yields in the four Timepix3 detectors at a pressure of the deuterium gas of 500 mbar, normalized to the highest yield in detector no. 2, obtained using fission barriers from Sierk scaled down by factor 0.85 (solid line) and 1.00 (dotted line). The fission neutron multiplicity was two. Experimental values are shown as symbols, error bars represent statistical errors.

In addition to the relative yields, Table I shows the total neutron yields in detector no. 2 for the two different gas pressures, for simulations with two values $C = 0.85$ and $C = 1.00$ for the scaling of the total fission barrier height and for the experimental values.

Again the simulation scaled down by 15% shows better agreement with experiment; this time, however, the main discrepancy in the simulation with full fission barriers is seen at the lower pressure of 500 mbar. The beam integral (5.4×10^{10} ions for 500 mbar and 7.7×10^{10} ions for 800 mbar) was obtained using the total yield of detected particles in the Timepix3 detectors (x rays, γ rays, and secondary electrons), normalized to sample rate provided by accelerator readings. While the data in Table I show absolute values for detector no. 2, where the neutron yield is largest, in combination with relative yields shown in Figs. 4 and 5 one can verify

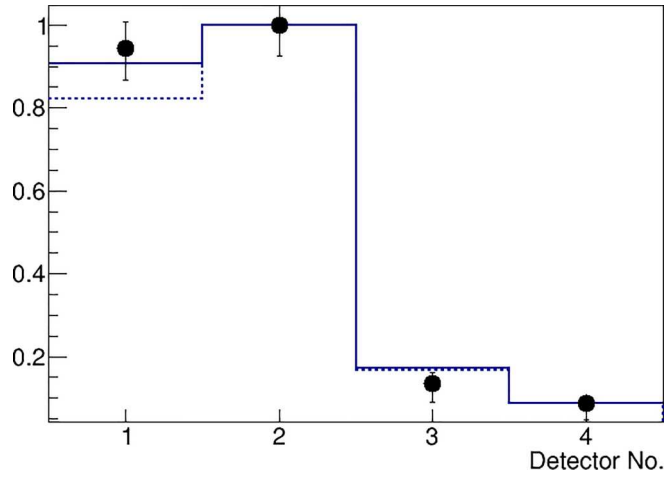

FIG. 5. Same as Fig. 4 for a pressure of the deuterium gas of 800 mbar.

TABLE I. Neutron yields for detector no. 2 for the two different gas pressures and for simulations with two values $C = 0.85$ and $C = 1.00$ for the scaling of the total fission barrier height and for the experimental values. The collected beam integral is 5.4×10^{10} ions for 500 mbar and 7.7×10^{10} ions for 800 mbar.

Gas pressure	$C = 0.85$	$C = 1.00$	Exp.
500 mbar	181	144	191 ± 14
800 mbar	238	218	228 ± 15

that simulation reproduced yields also in other detectors. As mentioned above, calculation with TALYS was performed with recommended set of parameters and it appears to reproduce the data. If the (d, p) and (d, n) cross sections from TALYS would be, e.g., larger or smaller by 10%, the simulation would fail since there would not be any parameter set which would reproduce experimental data both in Figs. 4, 5 and in Table I.

The success of the simulation demonstrates that the neutron yields and their spatial distributions carry the information about the spatial distribution of fission events in the gas volume, which represents the fission excitation function within the range of beam energies in the gas volume. Hence, the method presented here can be considered as fully capable of measuring the fission barrier heights of heavy unstable nuclei. Furthermore, the method can be regarded as a direct one, since the detected neutrons are the direct products of fission, just like fission fragments are. Figure 6 shows again the results of the successful simulation for 800 mbar pressure, together with the calculated neutron yield from the (d, n) process, which can be considered as a background process. It is clear that especially the neutron yield at forward angles cannot be reproduced without including the fission neutron yield from both (d, pf) and (d, nf) channels, a direct probe

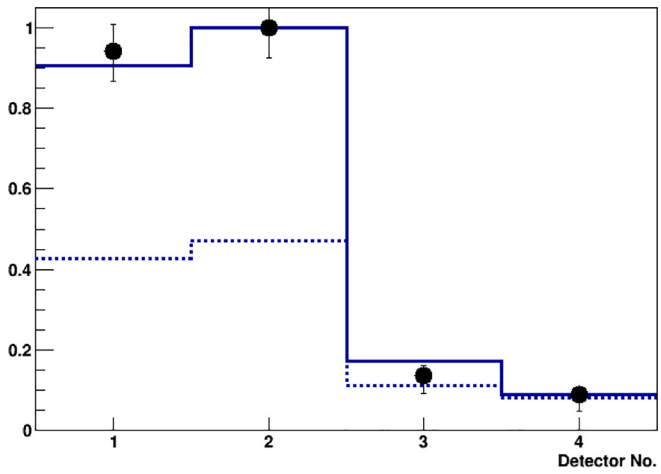

FIG. 6. Relative neutron yields in the four Timepix3 detectors at a pressure of the deuterium gas of 800 mbar, normalized to the highest yield in detector no. 2, obtained using fission barriers from Sierk scaled down by factor 0.85. The fission neutron multiplicity was two. The solid line shows the total neutron yield and the dotted line shows the yield of neutrons from the (d, n) process. Experimental values are shown as symbols, error bars represent statistical errors.

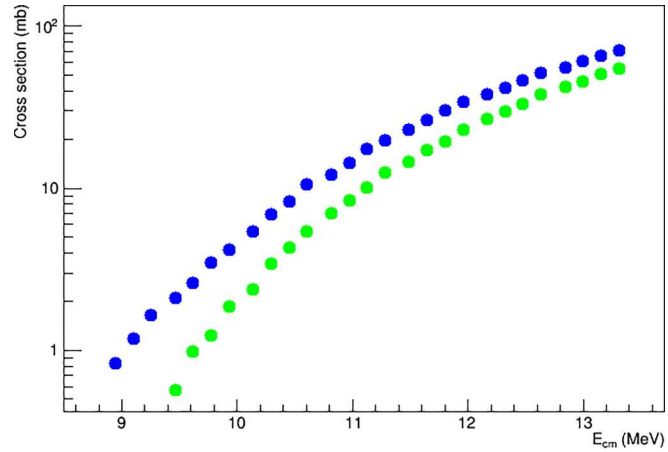

FIG. 7. Estimated cross sections of (d, pf) and (d, nf) fission channels (blue and green circles, respectively), obtained using fission barriers from Sierk scaled down by factor 0.85 and a fission neutron multiplicity of two.

related to fission cross section. In future experiments we plan to cover this region in more detail, thus increasing the overall sensitivity.

The successful simulation appears to describe well the fission probabilities and it also allows to estimate the experimental fission cross sections, relative to the (d, p) and (d, n) cross sections given by the TALYS code. Even if the [TALYS code with default parameters was used as initial guess, with the possibility to eventually scale the cross sections up or down, ultimately there was no need for such modifications. The resulting fission cross sections are shown in Fig. 7. The corresponding fission barrier heights are $B_f(^{210}\text{Fr}) = 10.67$ MeV and $B_f(^{210}\text{Ra}) = 8.54$ MeV. The uncertainty of these values amounts to 5%, which was the step used in simulations chosen to exceed the experimental statistical uncertainty. These values correspond to Sierk fission barriers, corrected for ground state shell corrections, and scaled down by 15%. When assuming macroscopic fission barrier of Cohen, Plasil, and Swiatecki [8], the full fission barrier needs to be scaled down by 20%. When restricting scaling only to macroscopic part of the fission barrier, the reduction is 25% for the macroscopic fission barrier of Sierk and 30% for the macroscopic fission barrier of Cohen, Plasil, and Swiatecki. The necessary values of barrier reduction are even higher for fission barriers of Möller *et al.* [10] (35% for ^{210}Fr and 30% for ^{210}Ra). Thus the reduction of the fission barrier height, reported in reactions leading to the competition of evaporation and fission in extremely neutron-deficient Fr and Ra isotopes at higher excitation energies [23,24], appears to be confirmed within experimental uncertainty in the present direct measurement of low-energy fission. Furthermore, the value of the pairing gap at 50% of the ground state value for ^{210}Ra also validates the results of the work of Ref. [11] for the even-even nucleus ^{180}Hg, for which a similar reduction of the fission barrier height was reported.

In the future, it is planned to continue measurement of fission barrier height for neutron-rich Fr isotopes, possibly ^{226}Fr. Such measurement will be much more challenging and

more detailed measurement of neutron angular distribution will be necessary due to larger background from (d, n) reaction. When successful, this measurement will allow to further verify the method by comparison with the already known fission barrier height of neutron-rich radium isotopes such as ^{226}Ra.

IV. CONCLUSIONS

We investigated the low-energy fission of ^{210}Fr and ^{210}Ra, produced in (d, p) and (d, n) transfer reactions in inverse kinematics with a beam of ^{209}Fr nuclei. Four Timepix3 pixel detectors were installed on the body of the ACTAR Demonstrator chamber with polyethylene converters for the detection of fast neutrons. Yields of fast neutrons from interactions of the the impinging beam with nuclei of the deuterium gas were measured at two gas pressures 500 and 800 mbar. No significant background was observed and thus it was possible to investigate the spatial distribution of emitted neutrons. Simulations employing the results of the TALYS code and available data on fission fragment distributions allowed to estimate directly the value of the fission barrier heights for the neutron-deficient nuclei ^{210}Fr and ^{210}Ra. Such a measurement, first of a kind and most suitable for very proton-rich nuclei, confirmed the reduction of the fission barrier compared to available theoretical calculations [8–10] by 15% to 30% for such extremely neutron-deficient unstable nuclei.

ACKNOWLEDGMENTS

Authors thank to the HIE-ISOLDE team for excellent beam. This work was supported by the Czech Science Foundation (GACR Contract No. 21-24281S); by the European Union's Horizon 2020 research and innovation programme under the Marie Skłodowska-Curie grant agreement FiBRa – no. 101025651; and by the Fonds de la Recherche Scientifique (F.R.S.-FNRS) and the Fonds Wetenschappelijk Onderzoek-Vlaanderen (FWO) under the EOS Projects No. 30468642 and No. 40007501. A.H. would like to thank the Slovak Research and Development Agency for support under Contract No. APVV-20-0532, and the Slovak grant agency VEGA (Contract No. 2/0067/21).

[1] I. V. Panov *et al.*, Nucl. Phys. A **747**, 633 (2005).
[2] M. Eichler *et al.*, Astrophys. J. **808**, 30 (2015).
[3] S. A. Giuliani, G. Martínez-Pinedo, M. R. Wu, and L. M. Robledo, Phys. Rev. C **102**, 045804 (2020).
[4] M. Dahlinger, D. Vermeulen, and K.-H. Schmidt, Nucl. Phys. A **376**, 94 (1982).
[5] K.-H. Schmidt *et al.*, Nucl. Phys. A **693**, 169 (2001); **665**, 221 (2000).
[6] A. N. Andreyev *et al.*, Phys. Rev. Lett. **105**, 252502 (2010); J. Elseviers *et al.*, Phys. Rev. C **84**, 034307 (2011).
[7] B. I. Pustylnik, Fiz. Elem. Chastits At. Yadra **31**, 273 (2000) [Phys. Part. Nucl. **31**, 129 (2000)].
[8] S. Cohen, F. Plasil, and W. J. Swiatecki, Ann. Phys. **82**, 557 (1974).
[9] A. J. Sierk, Phys. Rev. C **33**, 2039 (1986).
[10] P. Möller, A. J. Sierk, T. Ichikawa, A. Iwamoto, R. Bengtsson, H. Uhrenholt, and S. Aberg, Phys. Rev. C **79**, 064304 (2009).
[11] M. Veselský, A. N. Andreyev, S. Antalic, M. Huyse, P. Möller, K. Nishio, A. J. Sierk, P. Van Duppen, and M. Venhart, Phys. Rev. C **86**, 024308 (2012).
[12] Y. Kadi, Y. Blumenfeld, W. Venturini Delsolaro, M. A. Fraser, M. Huyse, A. Papageorgiou Koufidou, J. A. Rodriguez, and F. Wenander, J. Phys. G: Nucl. Part. Phys. **44**, 084003 (2017).
[13] T. Roger *et al.*, Nucl. Instrum. Methods Phys. Res. A **895**, 126 (2018).
[14] T. Poikela *et al.*, J. Inst. **9**, C05013 (2014).
[15] C. Granja, R. Uhlar, I. Chuprakov, P. Alexa, E. Sansarbayar, Y. M. Gledenov, D. Poklop, V. Olsansky, L. Marek, M. Vuolo, and J. Pacik, J. Inst. **18**, P01003 (2023).
[16] P. Burian *et al.*, J. Inst. **12**, C11001 (2017).
[17] L. Meduna, B. L. Bergmann, P. Burian, P. Mánek, S. Pospíšil, and M. Suk, in *Proceedings of the Connecting the Dots and Workshop on Intelligent Trackers* (CTD/WIT 2019).
[18] J. F. Ziegler, M. D. Ziegler, and J. P. Biersack, Nucl. Instrum. Methods Phys. Res. B **268**, 1818 (2010).
[19] A. J. Koning, S. Hilaire, and M. C. Duijvestijn, in *Proceedings of the International Conference on Nuclear Data for Science and Technology - ND2004* (AIP, 2005), Vol. 769, p. 1154.
[20] P. Moller, J. R. Nix, W. D. Myers, and W. J. Swiatecki, At. Data Nucl. Data Tables **59**, 185 (1995).
[21] C. Bockstiegel, Bestimmung der totalen kinetischen Energien in der Niederenergiespaltung neutronenarmer radioaktiver Isotope, Ph.D. thesis, TU Darmstadt, 1997, https://www-windows.gsi.de/Charms/theses.htm.
[22] P. Rubovič, D. Ekendahl, Z. Vykydal, J. Hulka, B. Bergmann, S. Pospíšil, and I. Stekl, Radiation Measurements **119**, 22 (2018).
[23] A. N. Andreyev *et al.*, Nucl. Phys. A **620**, 229 (1997).
[24] A. N Andreyev *et al.*, Nucl. Phys. A **626**, 857 (1997).